Structural Engineering and Mechanics, Vol. 6, No. 1 (1998) 95-113
DOI: http://dx.doi.org/10.12989/sem.1998.6.1.095

Static and dynamic finite element analysis of honeycomb sandwich structures

Matt H. Triplett† and William P. Schonberg‡

Civil and Environmental Engineering Department, The University of Alabama in Huntsville, Huntsville, Alabama 35899, U.S.A.

Abstract. The extensive use of honeycomb sandwich structures has led to the need to understand and analyze their low velocity impact response. Commercially available finite element software provides a possible analysis tool for this type of problem, but the validity of their material properties models for honeycomb materials must be investigated. Three different problems that focus on the effect of differences in honeycomb material properties on static and dynamic response are presented and discussed. The first problem considered is a linear elastic static analysis of honeycomb sandwich beams. The second is a nonlinear elastic-plastic analysis of a circular honeycomb sandwich plate. The final problem is a dynamic analysis of circular honeycomb sandwich plates impacted by low velocity projectiles. Results are obtained using the ABAQUS final element code and compared against experimental results. The comparison indicates that currently available material properties models for honeycomb materials can be used to obtain a good approximation of the behavior of honeycomb sandwich structures under static and dynamic loading conditions.

Key words: finite element analysis; honeycomb sandwich structures; low relocity impact; ABAQUS.

1. Introduction

Sandwich structures are used extensively in aircraft and military vehicles due to their light weight and high stiffness. Sandwich construction generally consists of thin high strength face plates bonded to a low density low strength core. Face materials vary from traditional metallic materials such as steel and aluminum to many types of fiber reinforced plastics. Soft low density materials such as honeycomb or foam can be used as core materials. The extensive use of honeycomb sandwich structures in such applications has led to the need to more fully understand and to better analyze their low velocity impact response. This type of analysis is especially useful for evaluation of vehicle crash vulnerability. Commercially available general purpose finite element software packages provide a possible simulation tool for this type of problem, but the validity of their material properties models for honeycomb materials must be investigated.

Analytical solutions for various static sandwich construction composite problems have been obtained by many investigators. Likewise, low velocity impact on sandwich structures has also been the subject of numerous investigations by analytical, experimental and numerical methods (see, e.g. Goldsmith and Louie 1995). Interestingly enough, the solution techniques employed in the analytical and numerical studies failed to address how the material constants for the

† Graduate Student
‡ Professor

honeycomb filler were obtained. Experimentally, transverse shear moduli are typically obtained using a rail shear test (Kuenzi 1957, Stevens and Kuenzi 1962, Kuenzi and Jenkinson 1974). Yield and ultimate strength, as well as stress strain curves, were also obtained by Kuenzi (1957) and Stevens and Kuenzi (1962). Analytical formulations for the upper and lower limits of the transverse shear moduli have been published by Kelsey, *et al.* (1958) and by Gibson and Ashby (1988). A finite element determination of these moduli based on upper and lower limits has been proposed by Grediac (1993). Formulations for the in-plane moduli and yield strengths have been determined analytically by Gibson, *et al.* (1982) and by Gibson and Ashby (1988), Gibson, *et al.* (1989) also developed in plane failure surfaces due to biaxial loading.

This paper considers three problems that focus on the modeling of honeycomb material properties. Of special interest is the effect of differences in material properties obtained using different methods on the predicted response of a particular type of honeycomb sandwich beam. The response predictions were obtained using the ABAQUS (HKS 1993) finite element code. First order solid elements were used throughout the analysis for the following reasons.

In general, linear elastic finite element analysis of composite beams and plates can be accomplished using shear deformation shell elements. These elements ignore stresses through the thickness of the beam or plate but do not account for transverse shear stress. These elements are appropriate for laminated composite and/or thick plate analysis where the transverse shear deformation cannot be ignored. However, no suitable shell element has been developed for elastic/perfectly-plastic material models where the transverse shear is included in the yield criteria. When transverse shear yield must be taken into account, solid elements must be used. First order elements do not perform well in bending without a very fine mesh (HKS 1993). Second order elements perform much better than first order elements as do incompatible mode elements if the mesh is rectangular (HKS 1993). However, if an analysis involved contact, second order elements should be avoided due to the numerical difficulties associated with ABAQUS contact algorithms (HKS 1993). When large deformations occur and solid elements are no longer rectangular, the incompatible mode elements do not provide an accurate solution (HKS 1993). Hence, for these reasons, first order solid elements were used in the finite element analyses performed as part of this study.

The first problem considered is concerned with various methods of obtaining elastic constants for honeycomb materials and their effect on static response. The magnitudes of the differences in response are evaluated by comparing available experimental response data to the predictions of linear static finite element analyses (FEA). The second problem focuses on inelastic deformation of honeycomb sandwiches. Again, the effect of using different methods to obtain yield constants for an elastic perfectly plastic material model is evaluated by performing a nonlinear FEA. The FEA results are compared to published experimental data for the quasi-static loading of a honeycomb sandwich plate. The third problem makes use of the material properties and models from the first two problems to analyze the low velocity impact of honeycomb sandwich plates where large and permanent deformations cannot be neglected. The FEA results are again compared to available experimental data.

2. Static linear elastic analysis

2.1. Introductory comments

Static finite element analyses are performed using both experimentally and analytically/numerically determined transverse shear moduli. The results of the analyses are compared against experimental test results. It will be shown that the transverse shear moduli are by far the most critical elastic constants for bending of honeycomb sandwich beams. Hence, they are the focus in this part of the investigation. The following section presents the analytical and numerical tools that are available to approximate the linear elastic constants required to describe a honeycomb material. These constants will be used for FEA of honeycomb sandwich beams, the results of which will then be compared to published experimental data.

2.2. Elastic constants

Fig. 1 shows a standard hexagonal honeycomb configuration and the coordinate system used throughout this investigation. Such a material is typically said to be orthotropic in nature; hence, there are nine effective elastic constants that need to be determined. These are E_1, E_2, E_3, ν_{12}, ν_{13}, ν_{23}, G_{12}, G_{13}, and G_{23}. Consider one cell as shown in Fig. 2. The cell shown is constructed of an isotropic material with modulus of elasticity E_c, Poisson's ratio ν_c, and shear modulus G_c (the c subscript indicates property of honeycomb constituent material). This cell geometry is typical of aluminum honeycomb construction where corrugated aluminum strips of thickness t are bonded together forming a honeycomb with vertical walls that have a thickness $2t$. Gibson and Ashby (1988) have presented the following analytical equations for the moduli E_1 and E_2 with uniform thickness t:

$$E_1=\left(\frac{t}{a}\right)^3\frac{(b/a+\sin\theta)}{\cos^3\theta}E_c \tag{1}$$

$$E_2=\left(\frac{t}{a}\right)^3\frac{\cos\theta}{(b/a+\sin\theta)\sin^2\theta}E_c \tag{2}$$

Eqs. (1) and (2) are obtained using standard beam theory to evaluate forces and deformations of the inclined walls. The formulation used to obtain E_1 and E_2 assumes that only inclined cell wall bending needs to be considered (i.e., the vertical walls with thickness '$2t$' do not contribute). For regular hexagonal cells where $\theta=30'$ and $a=b$, and both moduli are given by

$$E_1=E_2=\frac{4}{\sqrt{3}}\left(\frac{t}{a}\right)^3E_c \tag{3}$$

To calculate E_3, a modification to the formulation by Gibson and Ashby (1988) to include the thickness $2t$ as shown in Fig. 2 is done by considering a portion of the honeycomb cell as shown in Fig. 3. Based on the geometry in Fig. 3, the modulus E_3 is given by

$$E_3=\frac{t}{a}\left(\frac{1+b/a}{\cos\theta(\sin\theta+b/a}\right)E_c \tag{4}$$

For regular hexagonal cells,

$$E_3=\frac{t}{a}\left(\frac{8}{3\sqrt{3}}\right)E_c \tag{5}$$

The 1-2 Poisson's ratio is approximated by Gibson and Ashby (1988) based on the deflections due to inclined wall bending that were used to determine E_1 and E_2 and is given by

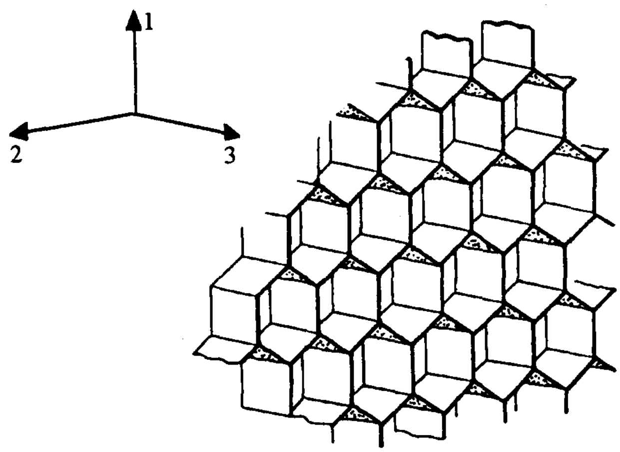

Fig. 1 Hexagonal honeycomb and coordinate system.

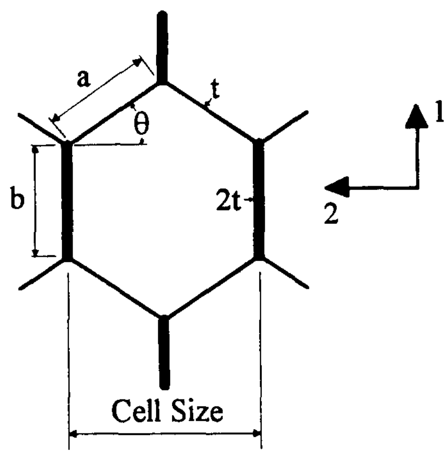

Fig. 2 Honeycomb cell.

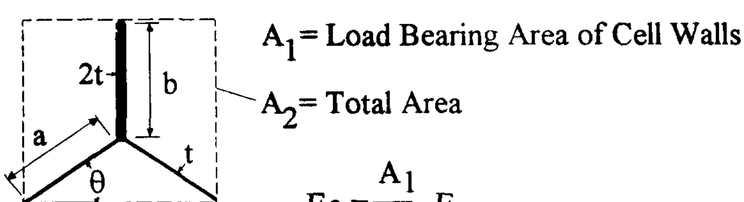

$$E_3 = \frac{A_1}{A_2} E_c$$

Fig. 3 Portion of honeycomb cell for E_3 formulation.

$$\nu_{12}=\frac{(b/a+\sin\theta)\sin\theta}{\cos^2\theta} \tag{6}$$

We note that $\nu_{12}=1$ for regular hexagons (i.e., $\theta=30°$ and $a=b$) and that ν_{12} in general is independent of wall thickness. Poisson's ratios ν_{31} and ν_{32} are simply the Poisson's ratio of the honeycomb material itself, ν_c (Gibson and Ashby, 1988). Using the reciprocal relation between moduli and Poisson's ratios in tensor notation, that is,

$$\frac{\nu_{ij}}{E_i}=\frac{\nu_{ji}}{E_j} \tag{7}$$

together with the above definition of ν_{31} and ν_{32} yields

$$\nu_{13}=\frac{E_1}{E_3}\,\nu_c\approx 0 \tag{8}$$

$$\nu_{23}=\frac{E_2}{E_3}\,\nu_c\approx 0 \tag{9}$$

The shear modulus G_{12} was also formulated analytically by Gibson and Ashby (1988). This formulation was done assuming the shear deflection is due entirely to cell wall bending so that standard beam formulas can be used to calculate the shear stress and strain, thus obtaining the shear modulus. As with the formulation of E_3, Gibson and Ashby considered the cell walls parallel to the 1-direction to have a thickness t. Fig. 4 shows the formulation method of Gibson and Ashby modified to consider the 1-direction wall thickness to be $2t$. Using standard beam equations, Gibson and Ashby arrived at the following expression for G_{12}:

$$G_{12}=\left(\frac{t}{a}\right)^3\frac{(b/a+\sin\theta)}{(b/a)^2(1+b/4a)\cos\theta}E_c \tag{10}$$

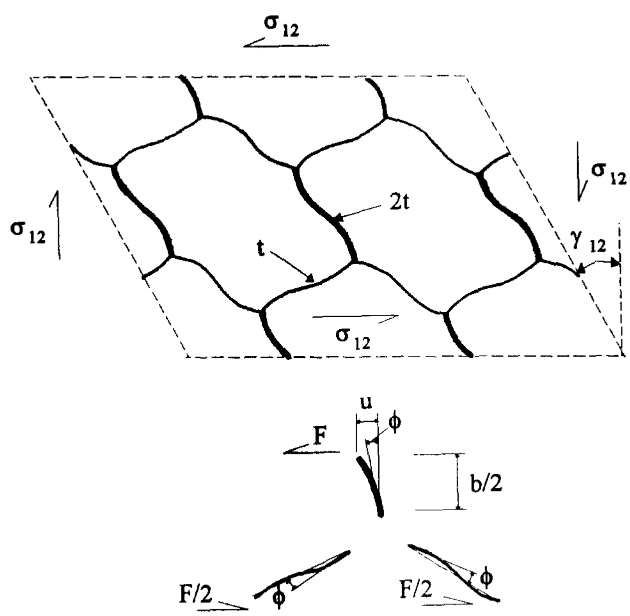

Fig. 4 Cell walls bending in 1-2 shear.

For regular hexagons Eq. (10) becomes

$$G_{12}=\left(\frac{t}{a}\right)^3 \frac{12}{5\sqrt{3}} E_c \tag{11}$$

For bending analysis of honeycomb sandwich structures, the transverse shear moduli (G_{13} and G_{23}) of the honeycomb are more important than the other honeycomb moduli. This is due to the fact that the transverse shear moduli are generally hundreds of times larger than the other moduli (except for E_3 which is even larger than the transverse shear moduli but not as critical unless through the thickness deformation is important). The analytical determination of transverse shear moduli is more complicated, but upper and lower bounds can be evaluated by using the theorems of minimum potential and minimum complementary energy (Kelsey, *et al.* 1958). Using minimum potential energy and a compatible strain field, the upper bound can be determined. The lower bound is found by using minimum complementary energy and a compatible stress field. If the two bounds are equal, an exact value is obtained (which is in fact the case for G_{23}). The transverse shear values, considering the cell walls parallel to the 1-direction have a thickness $2t$ as shown in Fig. 2, were analytically determined by Kelsey, *et al.* (1958) and are

$$\frac{(b/a)+\sin\theta}{(1+a/b)\cos\theta}\left(\frac{t}{b}\right)G_c=G_{13}^{lower}\leq G_{13}\leq G_{13}^{upper}=\frac{(b/a)+\sin^2\theta}{(1+(a/b)\sin\theta)\cos\theta}\left(\frac{t}{b}\right)G_c \tag{12}$$

$$G_{23}=\frac{\cos\theta}{1+(a/b)\sin\theta}\left(\frac{t}{b}\right)G_c \tag{13}$$

A finite element study of transverse shear in honeycomb materials (Grediac 1993) provides an approximation for G_{13} as a function of the upper and lower bounds given in Eq. (12) that was obtained using a least squares fit of finite element solutions for numerous cell configurations. This approximation is given as follows:

$$G_{13}=G_{13}^{lower}+.787\frac{a}{h}\left(G_{13}^{upper}-G_{13}^{lower}\right) \tag{14}$$

where 'h' is the thickness of the honeycomb core in the 3-direction.

2.3. Description of experiments and FEA model

Published experimental data concerned with bending of honeycomb sandwich structures is limited; only a small number of honeycomb sandwich beam bending experiments have been performed (Lingaiah and Suryanarayana 1991, Mines, *et al.* 1994). This section describes the experiments and the finite element model used in this investigation.

The experimental beam configurations are represented in Fig. 5, the dimensions are given in Table 1. The honeycombs used in each experiment have the configuration of Fig. 2 (i.e., parallel cell walls have thickness '$2t$'), are regular hexagons (i.e., $\theta=30°$ and $a=b$), and are constructed of 5052 aluminum; the only variation of the honeycomb in the three experiments is the wall thickness 't'. The experimental data for each case was presented as load and displacement at the center of the beams (Lingaiah and Suryanarayana 1991, Mines, *et al.* 1994). Due to the loading and geometric symmetry shown in Fig. 5, only half of the beams were modeled for the finite element analysis; each half contained 983 elements with 999 nodes, including the

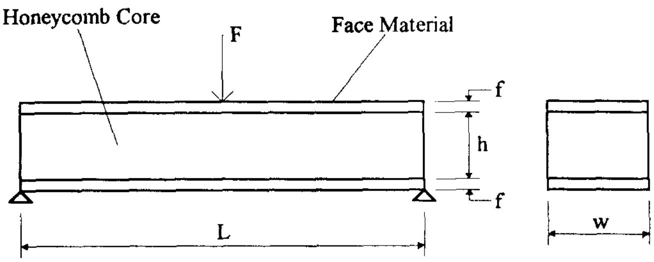

Fig. 5 Linear elastic static analysis: Experimental beam configuration.

Table 1. Linear elastic static analysis: Experimental beam dimensions (Honeycomb core cell wall material···5052-H32 Aluminum)

Reference	Face material	Honeycomb core cell size (cm)	*t* (cm)	*L* (cm)	*w* (cm)	*f* (cm)	*h* (cm)
Lingaiah and Suryanarayana (1991)	Unidirectional fiberglass	0.635	0.01	15.0	5.0	0.13	1.9
Mines, *et al.* #1(1994)	Woven fiberglass	0.635	0.006	40.0	6.0	0.055	1.3
Mines, *et al.* #2(1994)	Woven fiberglass	0.635	0.006	40.0	6.0	0.055	2.5

Table 2 Linear elastic static analysis: Material constants used for finite element analysis

	Lingaiah and Suryanarayana (1991)		Mines, *et al.* #1 (1994)		Mines, *et al.* #2 (1994)	
	Face*	Core	Face*	Core	Face*	Core
E_1 (GPa)	55.6	3.44×10^{-3}	20	0.84×10^{-3}	20	0.84×10^{-3}
E_2 (GPa)	17.9	3.44×10^{-3}	20	0.84×10^{-3}	20	0.84×10^{-3}
E_3 (GPa)	17.9	2.98	20	1.87	20	1.87
ν_{12}	0.25	1	0.11	1	0.11	1
ν_{13}	0.25	0	0.11	0	0.11	0
ν_{23}	0.25	0	0.11	0	0.11	0
G_{12} (GPa)	8.96	2.06×10^{-3}	4.13	0.50×10^{-3}	4.13	0.50×10^{-3}
G_{13c} (GPa)		0.65		0.41		0.40
G_{13e} (GPa)	8.96	0.87	4.13	0.59	4.13	0.53
G_{23c} (GPa)		0.42		0.26		0.27
G_{23e} (GPa)	8.96	0.35	4.13	0.25	4.13	0.23

*The face material properties were not calculated analytically

interface elements and nodes. Table 2 contains the elastic constants used for the analysis. The honeycomb elastic constants shown are obtained using the methods from the previous section and from manufacturer's rail shear and compressive tests. In those cases where a honeycomb constant was obtained by two different methods, the constants calculated by an analytical method are indicated with a '*c*' subscript, while an '*e*' subscript denotes an experimentally obtained elastic constant. The face material properties are not the focus of this investigation; hence, these constants were not obtained using analytical methods and no values are shown for these constants with a '*c*' subscript. As can be seen in Table 2, the analytical/numerical values of G_{13}, which is the larger of the two transverse shear moduli, are consistently smaller than the experimental values. This agrees with the work of Kelsey, *et al.* (1958) who showed that rail shear tests do in fact over-estimate the transverse shear moduli of honeycomb materials. The comparison of the results obtained from a finite element analysis using both calculated and experimental shear moduli and experimental beam deflection data is presented and discussed in the next section.

2.4. Comparison of experimental data and FEA results

The deflections at the center of the beam obtained from finite element analyses, using calculated and experimental properties, are compared to experimental results in Table 3. The results show that, for the beam geometry and loading considered, using the transverse shear properties obtained by the rail shear tests in an FEA gives smaller deflections than using calculated transverse shear properties in an FEA. However, with the exception of the Lingaiah and Suryanarayana experiments, the differences between the two types of finite element analyses and the experimental results are very slight. The larger difference in the case of the Lingaiah and Suryanarayana beam can be explained by a number of considerations.

First, the beam in the Lingaiah and Suryanarayana experiment had a much smaller length-to-thickness ratio (6.94) when compared to the length-to-thickness ratio in either of the beams in the Mines experiments (28.4 and 15.3 for experiments #1 and #2, respectively). That is, the Lingaiah and Suryanarayana beam was more "stocky" than both of the Mines beams. Because shear effects are more prominent in beams with low length-to-thickness ratios, the FEA of such beams would be especially sensitive to the transverse shear moduli used. Second, as can be seen in Table 4, the ratios of central beam deflection to any one of the three primary honeycomb geometric parameters (cell size, wall thickness and core depth) were much larger for the two Mines beams when compared to the Lingaiah and Suryanarayana beam. One might say that the geometries of the honeycomb cells in the Mines beams were overwhelmed by the deflections induced by the loads in those cases. In the Lingaiah and Suryanarayana beam, the honeycomb material evidently provided substantial resistance to deformation. Not surprisingly, the agreement between the numerical predictions and the experimental results was closest for the Mines beams, where the periodic nature of the honeycomb material was, in effect, washed out by the deformation.

Based on these considerations, it appears that numerical codes may have a tendency to work better in modeling the response of honeycomb beams that are highly flexible and are expected to undergo significant bending deformations. In general, however, it can still be said that the

Table 3 Linear elastic static analysis: Comparison of FEA and experimental results for central beam deflection

	Force (N)	Experimental results (cm)	FEA results calculated properties	% Diff. from Exp. results	FEA results experimental properties	% Diff. from Exp. results
Lingaiah and Suryanarayana (1991)	1,957	0.035	0.030	−14.3	0.028	−20.0
Mines, *et al.* #1 (1994)	809	2.04	1.89	−7.4	1.88	−7.8
Mines, *et al.* #2 (1994)	1,668	0.94	1.03	9.6	1.02	8.5

Table 4 Linear elastic static analysis: Ratios of beam displacements to various honeycomb gpometric parameters

	Ratio of deflection to honeycomb core cell size	Ratio of deflection to honeycomb wall thickness	Ratio of deflection to honeycomb core depth
Lingaiah and Suryanarayana (1991)	0.0551	3.5	0.0184
Mines, *et al.* #1 (1994)	3.21	340	1.569
Mines, *et al.* #2 (1994)	1.48	157	0.376

results of this analysis indicate that the use of effective material properties, whether they are obtained from testing or are calculated analytically, in finite element analysis of honeycomb structures in bending provides results that compare relatively well with experimental data.

3. Static nonlinear elastic-plastic analysis

3.1. Introductory comments

Modeling plastic behavior in materials is much more complex than modeling linear elastic behavior. To reduce complexity, approximations to the actual stress strain curve are typically made. However, the study of elastic-plastic behavior of honeycomb materials has not received much attention to date. In this study, Hills orthotropic yield criteria (Hill, 1950) will be used in an elastic perfectly plastic material model to approximate permanent deformations in honeycomb materials. In this section, methods to determine these yield constants for honeycomb materials will be reviewed. Yield Constants Gibson and Ashby (1988) studied the inelastic behavior of honeycombs in the 1-2 plane. Fig. 6 shows the typical shape of the stress strain curve of a honeycomb fabricated from an elastic-plastic metal loaded in the 1 or 2-direction. The yielding is due to plastic hinges forming in cell walls and the steep rise is due to cell walls aligning or touching. The cell walls will not align or touch until strains become extremely large so it appears that elastic perfectly plastic behavior will be a reasonable approximation of actual material response. Gibson and Ashby (1988) presented an analytical formulation for σ_{y1} and σ_{y2}. The formulation assumes that plastic hinges form only in the inclined cell walls having thickness t as was shown in Fig. 2 (recall that the formulation of E_1 and E_2 is the same regardless of the thickness of the cell walls parallel to the 1-direction). The upper bound of the yield values can be found by equating work done by forces on cell walls to the plastic work done at the hinges. The lower bound can be determined by equating the maximum moment in the cell wall to the fully plastic moment. If the upper and lower bounds are equal the formulation is exact, which is in fact the case for σ_{y1} and σ_{y2}. The equations presented by Gibson and Ashby (1988) are

$$\sigma_{y1}=\left(\frac{t}{a}\right)^2\frac{1}{2\cos^2\theta}\sigma_{yc} \tag{15}$$

$$\sigma_{y2}=\left(\frac{t}{a}\right)^2\frac{1}{2\sin\theta(b/a+\sin\theta)}\sigma_{yc} \tag{16}$$

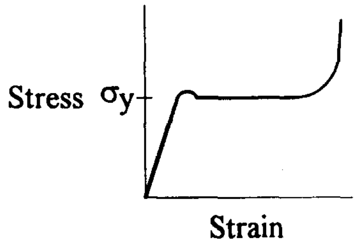

Fig. 6 Honeycomb stress strain curve in 1 or 2-direction.

For regular hexagonal honeycomb (i.e., $\theta=30°$ and $a=b$), σ_{y1} and σ_{y2} are equal and Eqs. (15) and (16) reduce to

$$\sigma_{y1}=\sigma_{y2}=\frac{2}{3}\left(\frac{t}{a}\right)^2\sigma_{yc} \tag{17}$$

where σ_{yc} is the yield stress of the honeycomb material.

Inelastic behavior of honeycomb materials in the 3-direction has been studied much more than that of other directions because honeycombs are often used as energy absorbers for compressive crushing in the 3-direction. The behavior of honeycomb in the 3-direction is different in tension and compression. Fig. 7 shows the typical shape of the compressive stress strain curve for a typical honeycomb. In Fig. 7, the curve drops to a uniform crush strength due to cell wall buckling. It is obvious that the stress strain behavior in tension would be quite different and have an ultimate strength considerably higher because of the absence of cell wall buckling. Unfortunately, material models in FEA codes have not been developed for this type of behavior. Hence, this study is forced to consider honeycomb behavior in tension to be the same as in compression.

The 3-direction yield value will be taken from the empirical formulation of ultimate compressive strength by Stevens and Kuenzi (1962) and is given by

$$\sigma_{y3}=45\,W^{5/3} \tag{18}$$

where W is the weight density in lbs/ft^3 and σ_{y3} has units of lbs/in^2. This formula is based on a curve fit of experimental data from aluminum honeycombs of various densities having regular hexagonal cells configured as shown in Fig. 2.

The yield value for shear in the 1-2 plane has been analytically formulated by Gibson and Ashby (1988) in a manner similar to the method used to determine σ_{y1} and σ_{y2}. It is assumed that the yielding is due to the formation of plastic hinges in the cell walls parallel to the 1-direction. The upper and lower bounds are equal as they are in the formulation of σ_{y1} and σ_{y2}, so the solution is exact. With the cell walls parallel to the 1-direction having a thickness '$2t$', the result of the analytical formulation is the equation

$$\sigma_{y12}=\left(\frac{t}{a}\right)^2\frac{1}{(b/a)\cos\theta}\sigma_{yc} \tag{19}$$

which reduces to

$$\sigma_{y12}=\frac{2}{\sqrt{3}}\left(\frac{t}{a}\right)^2\sigma_{yc} \tag{20}$$

for regular hexagonal cells.

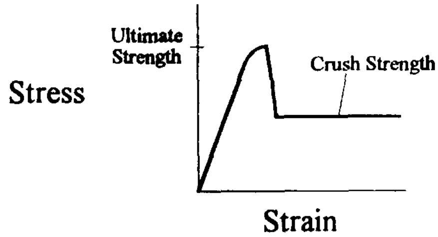

Fig. 7 Compressive honeycomb stress strain curve in 3-direction.

As was stated previously, even though the properties of honeycombs in transverse shear (shear in the 1-3 and 2-3 planes) are more critical than other properties, the inelastic behavior of honeycombs in transverse shear has received almost no attention. The shape of a typical stress strain curve in transverse shear is shown in Fig. 8 (Bitzer 1993). Stevens and Kuenzi (1962) provided the yield values as shown in Fig. 8 but did not provide any curve fit information. A linear regression analysis on the data presented by Stevens and Kuenzi was performed; a curve fit of this data produces the following relations

$$\sigma_{y13}=69\,W-62 \tag{21}$$

$$\sigma_{y23}=31\,W-17 \tag{22}$$

Once again, W is in lbs/ft^3 and the σ_{y13} and σ_{y12} are in lbs/ft^2. The analysis produces an R^2 value of 0.97 for Eq. (21) and 0.95 for Eq. (22). Due to the fact that no analytical studies of inelastic behavior in transverse shear are available, the empirical formulations in Eqs. (21) and (22) will be used to provide the yield constants for Hill's yield criteria.

3.3. Description of experiments and FEA model

Beckmann (1990) published results of an experiment in which a circular honeycomb sandwich plate was loaded quasi-statically and subsequently exhibited inelastic deformations. The results of this experiment will be compared against the results of a FEA using the elastic perfectly plastic approximation for the honeycomb material as presented in the previous section. This section describes the experiment and the finite element model used for this part of the study.

The experimental configuration, shown in Fig. 9, consisted of a circular plate with aluminum face plates and an aluminum honeycomb core. The plate diameter was 25 cm and simply supported around the outside edge continuously. Additional geometric parameters are given as indicated in Table 5. The load was applied quasi-statically through a projectile that was used for the impact experiments which will be discussed in a subsequent section. The projectile was an aluminum cylinder with a diameter of 7.5 cm and a steel head having a convex curvature with a 46 cm radius. The results of the experiment were presented as force and displacement at the center of the plate (Beckmann 1990).

The loading and geometry shown in Figure 9 are symmetric about the axis of the cylinder and plate, but the material properties of the honeycomb are not. A full three dimensional FEA would be required to account for the symmetry mismatch between the aluminum and the honeycomb material, but large computation times would be required. Instead, an axisymmetric approximation will be made by using a transversely isotropic material model. In such a material model, the elastic constants required are E_1, E_3, ν_{12}, ν_{13}, and G_{13}. Thus, the only modification to the

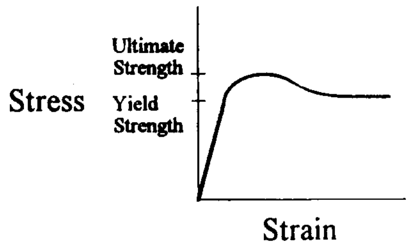

Fig. 8 Honeycomb transverse shear stress strain curve.

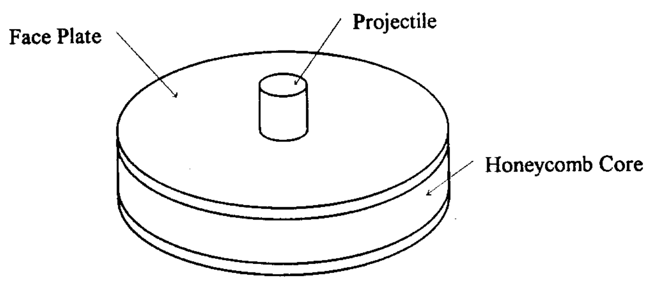

Fig. 9 Nonlinear elastic-plastic analysis: experimental plate configuration.

Table 5 Nonlinear elastic-plastic and dynamic analyses: Experimental plate configurations (face and honeycomb core cell wall material···5052-H32 aluminum)

Exp. No.	Honeycomb cell size (cm)	t (cm)	f (cm)	h (cm)	Projectile velocity (m/s)
			Elastic-plastic		
–	0.32	0.0025	0.08	1.9	–
			Dynamic		
1	0.32	0.0025	0.08	1.9	2.5
2	0.32	0.0050	0.08	1.9	3.0

analytical formulation of the effective elastic constants discussed previously is for transverse shear. The transversely isotropic shear modulus G_{13} will be approximated by using the average of the two orthotropic shear modulus values, that is

$$G_{13\text{-}eff}=(G_{13}+G_{23})/2 \tag{23}$$

Similarly, the orthotropic shear yield stress values are also averaged to yield the transversely isotropic approximation, that is,

$$\sigma_{y13\text{-}eff}=(\sigma_{y13}+\sigma_{y23})/2 \tag{24}$$

The finite element model consists of axisymmetric solid elements to represent the honeycomb and face materials and an axisymmetric rigid surface to approximate the projectile used to apply the load. As in the previous case, 983 elements with 999 nodes comprised the finite element model. The honeycomb material properties are given in Table 6. Note that in Table 6, E_1, E_3, ν_{12}, ν_{13}, and σ_{y1} were calculated using analytical formulations. However, $G_{13\text{-}eff}$, σ_{y3}, and $\sigma_{y13\text{-}eff}$

were calculated using empirical formulas because analytical formulations for these parameters have not yet been developed. The face material is 5052-H32 aluminum and modeled as an isotropic elastic perfectly plastic material. Only two elastic constants are needed; they can be obtained from MIL-HDBK-5F (1990) and are $E=70$ GPa, $\nu=0.33$. Finally, the von Mises yield criterion is used to determine the onset of plasticity; the yield value is $\sigma_y=155$ MPa (MIL-HDBK-5F, 1990).

3.4. Comparison of experimental data and FEA results

A plot of deflection at the center of the plate as a function of the load applied to the projectile is shown in Fig. 10 for both the FEA and the experimental results of Beckmann (1990). The sudden drop in the experimental curve at a deflection of 0.25 cm is most likely due to local core crushing. Post-experiment measurements made by Beckmann (1990) showed a top face deflection of 1.4 cm and a bottom face deflection of 1.2 cm, indicating 0.2 cm of core crushing. According to Beckmann (1990), the crushing of the honeycomb core appeared as buckling of the honeycomb walls under and in the immediate vicinity of the indenter. The permanent deformation of the top face plate as predicted by the FEA is 1.7 cm, which is 21% higher than the experimental value.

We note that because an elastic perfectly plastic material model was used in this investigation, the finite element analysis did not consider core crushing. Although the FEA results do not agree precisely with the experimental results, they do indicate that the use of Hill's yield criteria and an elastic perfectly plastic material model does provide a reasonable approximation of the behavior of honeycomb sandwich plates.

A possible reason for the lack of a more precise agreement in Fig. 10 can be the uncertainty of the proper value for shear yield stress shown in Fig. 8. For this reason, the FEA was performed using 110% and 120% of the value of $\sigma_{y13\text{-}eff}$ shown in Table 6 (i.e., 110% and 120% of the value obtained from Eq. (24)). A plot of deflection at the center of the plate as a function of the load applied to the projectile is shown in Fig. 11 for both the FEA (using 100%, 110%, and 120% of $\sigma_{y13\text{-}eff}$ and all other material constants as in Table 6) and the experimental results of Beckmann (1990). It appears that 110% of the $\sigma_{y13\text{-}eff}$ value shown in Table 6 may be a better value for the shear yield stress. However, additional tests should must be run to see if this conclusion can be generalized.

In Table 7, the maximum central displacement as predicted by the FEA is compared to the experimental value obtained by Beckmann (1990) for the non-linear elastic-plastic problem. As can be seen in this Table, there is excellent agreement between the numerical prediction and the experimental value. We note that the diameter-to-thickness ratio for the plate configuration considered by Beckmann is approximately 12.1; other ratio values of interest involving the maximum central displacement and the geometry of the honeycomb material for this problem are

Table 6 Nonlinear elastic-plastic analysis: Honeycomb material constants used for FEA

E_1 (GPa)	E_3 (GPa)	ν_{12}	$G_{13\text{-}eff}$ (GPa)	σ_{y1} (MPa)	σ_{y3} (MPa)	$\sigma_{y13\text{-}eff}$ (MPa)
0.44×10^{-3}	1.496	1	267	0.028	3.81	1.27

Note: E_1, E_3, ν_{12}, and σ_{y1} calculated using analytical formulations; $G_{13\text{-}eff}$, σ_{y3}, and $\sigma_{y13\text{-}eff}$ were calculated using empirical formulas.

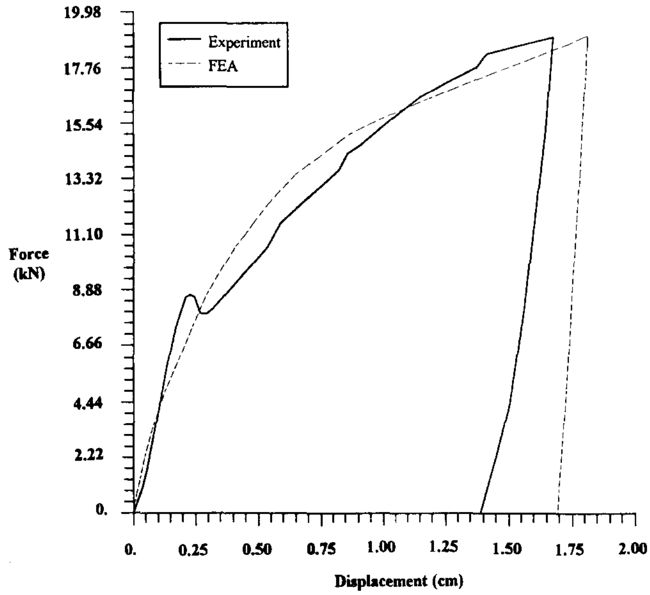

Fig. 10 Nonlinear elastic-plastic analysis: Force displacement of FEA and experiment.

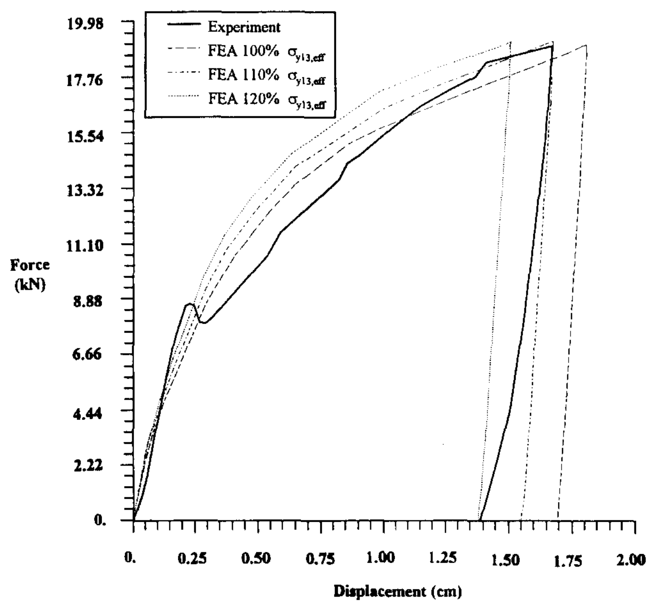

Fig. 11 Nonlinear elastic-plastic analysis: Force displacement of FEA (using three different values for $\sigma_{y13\text{-}eff}$) and experiment.

given in Table 8. The ratio values in Table 8 and the plate diameter-to-thickness ratio for this problem are similar to the corresponding values for the beams used by Mines *et al.* in performing a static linear elastic analysis. It is recalled that the numerical results agreed fairly well with the experimental data for these beams. Hence, considering the geometric similarity between the circular plate used by Beckmann and the beams used by Mines, it is not totally surprising to find that the numerical prediction for the problem under consideration also agrees well with

Table 7 Elastic-plastic and dynamic analyses: Comparison of FEA and experimental valuesof maximum central beam displacement (Beckman 1990)

	Experimental value (cm)	FEA value (cm)	% Diff. from Exp. results
Elastic-plastic problem	1.68	1.80	7.1
Dynamic problem #1	1.85	1.83	−1.1
Dynamic problem #2	1.85	1.90	2.7

Table 8 Elastic-plastic and dynamic analyses: Ratios of beam displacements to various honeycomb geometric parameters (Beckman 1990)

	Ratio of deflection to honeycomb core cell size	Ratio of deflection to honeycomb wall thickness	Ratio of deflection to honeycomb core depth
Elastic-plastic problem	5.25	672	0.884
Dynamic problem #1	5.78	740	0.974
Dynamic problem #2	5.78	370	0.974

the experimental result.

4. Dynamic impact analysis

4.1. Introductory comments

Beckmann (1990) also presented results of two experiments involving the low velocity impact of circular honeycomb sandwich plates which resulted in permanent deformations. The results of these experiments will be compared to dynamic FEA using the analytical and empirical formulations for elastic and plastic constants presented previously. Following a description of the experiments and the finite element model used for the dynamic investigation, a comparison of the experimental results and FEA predictions is presented and discussed.

4.2. Description of experiments and FEA model

The experimental configurations were the same as shown in Fig. 9 except that the sandwich plates were loaded by firing the projectile at low velocities. For the two experiments considered, the only variations were honeycomb cell wall thickness and the velocity of the projectile. A summary of the experimental configurations is presented as indicated in Table 5. As was the case in the quasi-static problem considered previously, the projectile was an aluminum cylinder with a diameter of 7.5 cm and a steel head having a convex curvature of a 46 cm radius. The experimental results were presented as projectile force versus displacement (Beckmann 1990).

As in the quasi-static problem, the low velocity problem under consideration was considered to be approximately axisymmetric which allowed the use of transversely isotropic properties for the honeycomb material. The honeycomb material properties used for the FEA are summarized in Table 9 and were obtained by the methods presented in the previous sections; the face material properties are as given previously. The finite element model used in the dynamic analysis consisted of 2085 elements with 2104 nodes, including the interface elements and nodes.

4.3. Comparison of experimental data and FEA results

Plots of the deflection at the center of the plate as a function of impact force are shown in Fig. 12 and 13 for Experiments 1 and 2, respectively. In Fig. 13 the impact force from the FEA rises much faster than the experimental results and has a significantly higher initial peak value. This difference can be explained by core crushing that is ignored in the FEA. In Experiment 1 (see Fig. 12), the honeycomb core thickness was reduced from 1.9 cm to 1.7 cm. This difference can also be seen in Fig. 13, but is not as pronounced because in Experiment 2 the honeycomb core thickness was only reduced by only 0.25 mm (i.e., only 1.3% as compared to 11% in Experiment 1). The core crushing in Experiment 1 is larger than Experiment 2 because the honeycomb core in Experiment 2 has thicker cell walls and therefore increased strength.

Another difference in the FEA verses experimental data comparisons is the oscillations in the FEA results that are not present in the experimental data. Part of this difference may be explained by the method by which the experimental data was obtained. In the experiments, the motion of the projectile was recorded by an optical sensor that measured displacements. The displacement as a function of time was then filtered and differentiated twice to obtain accelerations which were then multiplied by the projectile mass to obtain impact force as a function of time. This filtering and differentiation undoubtedly removed most or all of the oscillations. Additionally, no structural damping was used in the FEA which may also explain part of the difference in oscillations between the FEA and the experiments.

The data for Experiment 2 shows a drop in the force between 0.5 cm and 1.3 cm of displacement which is not present in the FEA results. A possible explanation for this difference may be localized crushing of the core at the support location or failure of the bond between the face plates and the honeycomb core. Neither of these were discussed in the publication by Beckmann nor were they modeled in the FEA.

In Table 7, the maximum central displacements as predicted by the FEA for the dynamic problems are compared to the values obtained experimentally by Beckmann (1990). As can be seen in the final two rows of this Table, there is again excellent agreement between the numerical predictions and the experimental values. Since the plates used in the dynamic problems are identical to the one used in the elastic-plastic problem, the diameter-to-thickness ratio is again approximately 12.1; other ratio values of interest involving the dynamic maximum central displacements and the geometries of the honeycomb material for this problem are given in the second and third rows of Table 8. Once again, the ratio values in Table 8 and the plate diameter-to-thickness ratio for this problem are similar to the corresponding values for the beams

Table 9 Dynamic analysis: Material constants used for FEA

Exp. No.	E_1 (GPa)	E_3 (GPa)	ν_{12}	$G_{13,eff}$ (GPa)	σ_{y1} (MPa)	σ_{y3} (MPa)	$\sigma_{y13,eff}$ (MPa)
1	0.44×10^{-3}	1.496	1	0.267	0.028	3.81	1.27
2	3.46×10^{-3}	2.993	1	0.535	0.113	10.14	2.47

Note: E_1, E_3, ν_{12}, and σ_{y1} calculated using analytical formulations; $G_{13,eff}$, σ_{y3}, and $\sigma_{y13,eff}$ were calculated using empirical formulas.

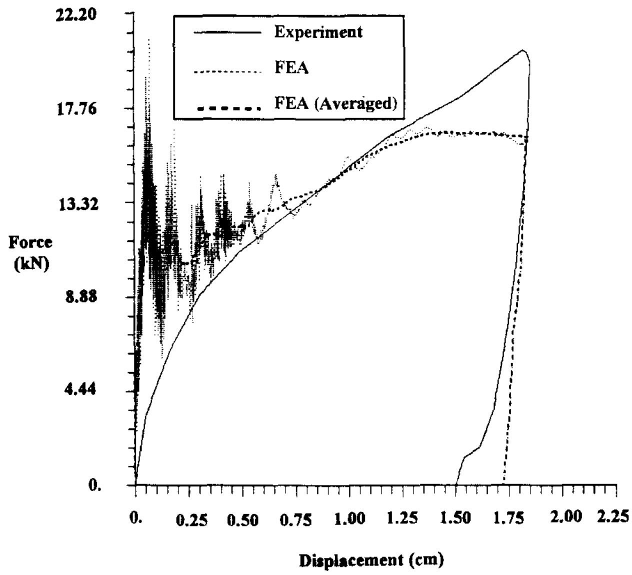

Fig. 12 Dynamic analysis: Force displacement of FEA and experiment 1.

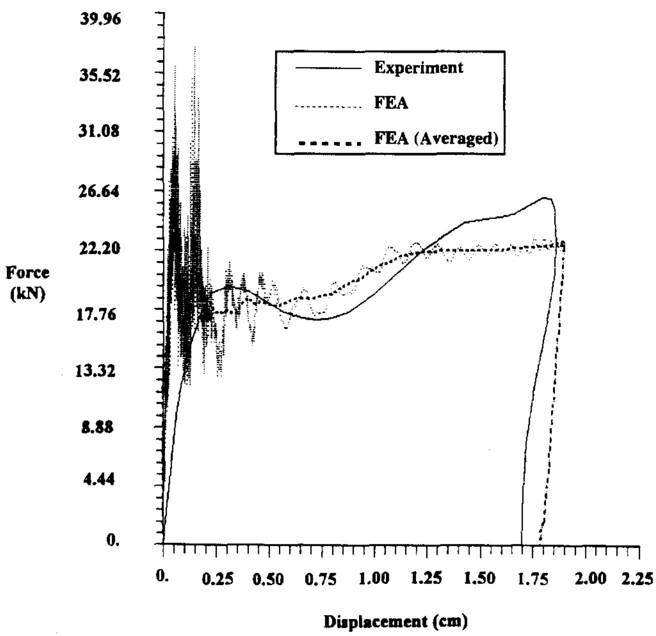

Fig. 13 Dynamic analysis: Force displacement of FEA and experiment 2.

used by Mines, et al. in performing a static linear elastic analysis. Hence, it is again not totally surprising to find that the numerical predictions for the problem under consideration also agree rather well with the experimental results.

Finally, the differences in final plate displacement between the FEA predictions and the experimental results are approximately 17% and 5% for Experiments 1 and 2, respectively. As was the case with the quasi-static problem, there is not a precise agreement between the experiment and the FEA, but the results do indicate that the methods used for finite element analysis in this investigation can provide a good approximation of honeycomb sandwich beam response to low velocity impact.

5. Conclusions and recommendations

The results of this investigation indicate that the use of empirical and calculated effective material constants for honeycomb can be used to provide a reasonable approximation of the behavior of honeycomb sandwich structures. These material constants can be use in conjunction with a linear elastic perfectly plastic material model and the finite element method to analyze the response of honeycomb sandwich structures to static and dynamic loads.

In the first part of this investigation analytical/numerical methods of determining linear elastic constants for honeycombs were presented. A static FEA was performed on honeycomb sandwich beams using both analytical/numerical elastic constants and experimentally determined constants. These FEA results were then compared to published experimental data. Of particular interest in this comparison is the effect of the transverse shear moduli because it is by far the most important property in the bending of honeycomb sandwich beams. Although there was not enough experimental beam data to determine which method of obtaining transverse shear moduli is better, the results do show that this difference is more important in beams with low length to thickness ratio (i.e., stocky beams). However, the results do indicate that the use of effective elastic constants, whether calculated or obtained by experiment, provide a reasonable approximation of honeycomb sandwich beam behavior.

The second part of this investigation focused on the inelastic behavior of honeycomb materials. Analytical and empirical methods of obtaining yield constants for honeycomb materials were presented. These yield constants and the elastic material properties presented in the first part of the investigation were used to perform a static FEA. The results of this FEA were compared to published quasi-static experimental data that included inelastic deformations. Although only one set of experimental data was available and the FEA results did not agree precisely with the experiment, the results do indicate that these analysis methods can be used to predict the overall response of honeycomb sandwich structures subject to inelastic deformations.

The third and final part of the investigation focused on the low velocity impact of honeycomb sandwich structures. The methods of obtaining material constants for an elastic perfectly plastic model presented in the first two parts of this investigation were used to perform dynamic FEA of circular honeycomb sandwich plates impacted by low velocity projectiles. A two dimensional analysis was needed for the dynamic analysis to keep computer run times to a minimum. Although the run time required for the static inelastic problem was only 13 minutes, the run time for the dynamic problems were approximately 200 hours. The large run times required for the dynamic analysis would preclude a full three dimensional analysis of a complex structure. As was the case for the static inelastic problem, an exact match to the experimental data was not obtained. The FEA did however predict the overall response relatively well. The results do indicate that the agreement between experiment and FEA gets worse as the amount of honeycomb core crushing increases because honeycomb crushing is ignored in the FEA model. The two dimensional FEA, as presented in this investigation, could be very useful in the evaluation of the energy absorbing capabilities of honeycombs with varying cell dimensions and materials (as long as the cell geometry is hexagonal and the material is isotropic).

Acknowledgments

The authors would like to thank the Structures Directorate of the United States Army Missile Command for the use of the computer resources that were required to complete this investigation.

References

Beckmann, W. (1990). "Dynamic energy absorption characteristics of edge-supported sandwich plates", in *Inelastic Deformation of Sandwich Plates and Shells Under Dynamic Loading* by W. Goldsmith and J. L. Sackman, University of California, Berkeley, AFSOR-TR-91-0233.

Bitzer, T. (1993). *Private Communication.* Hexcel Corporation, Dublin, California.

Gibson, L. J. and M. F. Ashby. (1988). *Cellular Solids Structure and Properties,* Pergamon Press, New York.

Gibson, L. J., M. F. Ashby, G. S. Schajer and C. I. Robertson. (1982). "The mechanics of two-dimensional cellular materials", *Proc. R. Soc. Lon.,* A382, 25-42.

Gibson, L. J., M. F. Ashby, J. Zhang and T. C. Triantafillou. (1989). "Failure surfaces for cellular materials under multiaxial loads - I. Modeling", *Int. J. Mech. Sci.,* **31**(9), 665-678.

Goldsmith, W. and D.L. Louie. (1995). "Axial perforation of aluminum honeycombs by projectiles", *Int. J. Solids Structures,* **32**(8/9), 1017-1046.

Grédiac, M. (1993). "A finite element study of the transverse shear in honeycomb cores", *Int. J. Solids Structures,* **30**(13), 1777-1788.

Hexcel Corp. (1992). *Mechanical Properties of Hexcel Honeycomb Materials,* TSB 120.

Hibbitt, Karlsson and Sorensen, Inc. (HKS). (1993). *ABAQUS Version 5.3 Theory Manual and Users Guide.*

Hill, R. (1950). *Plasticity,* Oxford University Press, England.

Kelsey, S., R. A. Gellatly and B. W. Clark. (1958). "The shear modulus of foil honeycomb cores", *Aircraft Engineering,* 294-302.

Kuenzi, E. W. (1957). *Mechanical Properties of Glass-Fabric Honeycomb Cores,* Forest Products Laboratory, Madison, Wisconsin, Report No. 1861.

Kuenzi, E. W. (1970). *Minimum Weight Structural Sandwich,* Forest Products Laboratory, Madison, Wisconsin, Report No. FPL-086.

Kuenzi, E. W. and P. M. Jenkinson. (1974). *Compressive and Shear Properties of Polyamide Honeycomb Core,* Forest Products Laboratory, Madison, Wisconsin, Report No. FPL-0202.

Lingaiah, K., and B. G. Suryanarayana. (1991). "Strength and stiffness of sandwich beams in bending", *Experimental Mechanics,* 1-7.

MIL-HDBK-5F. (1990). *Metallic Materials and Elements for Aerospace Vehicle Structures.*

Mines, R. A. W., C. M. Worrall and A. G. Gibson. (1994). "The static and impact behavior of polymer composite sandwich beams", Composites, **25**(2), 95-110.

Stevens, G. H. and E. W. Kuenzi. (1962). *Mechanical Properties of Several Honeycomb Cores,* Forest Products Laboratory, Madison, Wisconsin, Report No. FPL-1887.